Review on Comparison of Different OFDM Symbol Timing Synchronization Algorithms

Ravi Kant Gupta , Anuj Jain*

Bhagwant University,Ajmer, Rajasthan
ravikant_gupta2008@yahoo.com, akj_1112@rediffmail.com*

Abstract: Orthogonal Frequency Division Multiplexing (OFDM) is the key technology for 4G and 3GPP LTE systems due to its highly efficient bandwidth and multi carrier modulation. The benefit of using OFDM is that it avoids ISI (Inter Symbol Interference) and ICI (Inter carrier Interference) by using timing synchronization technique. For this the symbols must be in properly synchronized form. It also have Higher transmission rate. So SC (Schmidl and Cox) algorithm is designed, It provides timing synchronization and lowers BER(Bit Error Rate). Based on the research of Schmidl & Cox, Minn and Bhargava and Park et al. synchronization algorithm, this paper proposed a comparison on these three timing synchronization algorithms.

Keywords: OFDM, Orthogonal Frequency Division Multiplexing, Synchronization, BER, Timing Synchronization.

I.Introduction

The dramatic growth of voice, data, and video communications over the Internet fueled a demand for high data rates. Numerous techniques exist in order to meet the increasing demand. OFDM is at the center of these efforts due to its attractive features. The principle of OFDM is that it takes a data stream, and after multiplexing, sends the data over a range of sub-carriers, thus transmitting the data simultaneously over a number of different carriers. Each sub-carrier carries a portion of the data. This helps OFDM reach higher data rates without being affected by the channel distortions. The subcarriers are orthogonal to each other. This allows the sub-carriers to overlap in frequency with the adjacent carriers without causing interference. Another benefit of orthogonality is high spectral efficiency [i][ii]. Besides being better suited to overcome frequency selective fading and multi-path effects, OFDM also has implementation advantages, such as avoiding ISI and ICI, over other multi-carrier communication schemes. OFDM was chosen as the standard communication technique by many wired and wireless applications today. Among them are Asymmetric Digital Subscriber Line (ADSL), Digital Audio Broadcasting (DAB), and Digital Video Broadcasting (DVB). Most high speed wireless communication standards adopt OFDM or adopting OFDM for transmission e.g. IEEE 802.11, IEEE 802.16, IEEE 802.20, European Telecommunication Standards Institute, BRAN (Broadcast Radio Access Networks) committee [iii] [iv].
The block diagram of OFDM transceiver is given below:
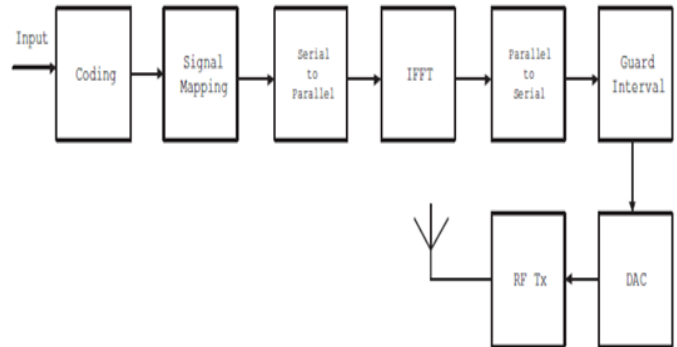Here Figure 1(A) shows the transmitter and Figure 1(B) shows the receiver.
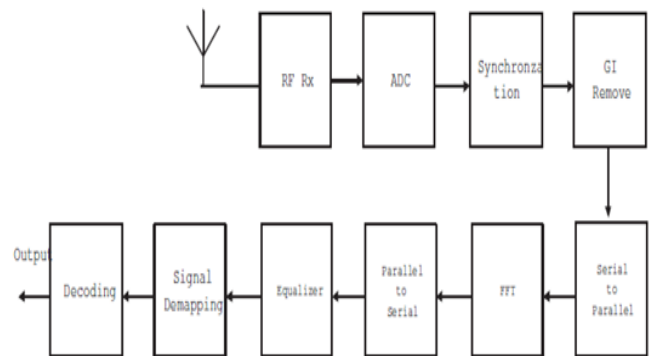

Figure 1(A) : Transmitter

Figure 1(B) : Receiver

Figure 1: Block diagram of OFDM Transceiver

OFDM system synchronization mainly includes three types of synchronization:

1. Timing synchronization
2. Carrier frequency synchronization
3. Sampling clock synchronization

First type (means timing synchronization) includes two parts :

i. Frame synchronization – It is used to determine the starting position of the Data packet.

ii. Symbol synchronization – It is used to determine the starting position of OFDM symbols Here timing synchronization ensures the accuracy of FFT (Fast Fourier Transform) transformation.

Now come to **second type** (means carrier frequency synchronization) which detect the frequency offset, and after that it will be compensated.

Now come to the **third** type (means sampling clock synchronization) which is used to eliminate the impact of the frequency deviation and phase deviation. Where frequency deviation is the value of difference between clock frequency at the receiving terminal and the sending terminal. The phase deviation is the value of difference between the phase at the receiving terminal and sending terminal. Here we talk about Timing synchronization in OFDM-based systems, the effects of timing errors, and the distortions caused by these errors.

II. Material and Methodology :

The Need For Timing Synchronizations and Timing Errors

At the OFDM receiver, the signal initially goes through a synchronization process before being demodulated into the frequency domain) as we seen in Figure1.Besides timing synchronization, the synchronization process also includes synchronization of the frequency, the sampling clock, and the phase. However, they are beyond the scope of this study. The very first process the signal goes through is the coarse timing or signal detection. The function of coarse timing is to detect the incoming signal and to activate the receiver for the data. The coarse timing is not precise enough to determine the actual start time of the symbols, so fine timing synchronization methods are required to determine the actual start time of the symbol. Fine timing is crucial to reduce both the ICI and ISI.

The purpose of the timing synchronization or the timing offset estimation is to find a starting point for the FFT operation at the receiver. The importance of the accuracy of such an estimate lies in the fact that ISI and ICI can be avoided. Figure 2 shows an illustration of where ISI and ICI might occur in an OFDM system.
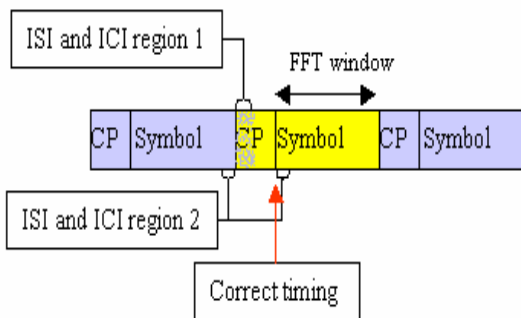

Figure 2. Illustration of ISI and ICI in OFDM Systems

The ISI and ICI may occur under two conditions, assuming that there are no frequency Errors.

The first condition is when we choose a sample close to the end of the CP as the correct starting point of the FFT window, i.e., early timing, due to multi-path. This type of ISI and ICI is illustrated as "ISI and ICI region 1" in Figure 2. When timing is estimated in this region, ISI and ICI occur due to the delayed versions of the previous OFDM symbol.

The second condition is when we choose a sample outside of the CP as the correct starting point, i.e., late timing. This type of ISI and ICI is illustrated as "ISI and ICI region 2" in Figure 2 having ISI from the previous symbol due to multi-path also causes ICI. The distortion caused by ICI in this case is negligible. In a non-coherent detection scheme, such as differential coding/decoding used, there will be some residual phase rotation due to ICI.

In such systems, a timing phase estimator [v, vi] could be used to detect and to correct the phase rotation caused by ICI. Figure 3 illustrates the effect of the ISI and ICI due to early synchronization, i.e, early timing, in terms of bit error rate versus bit energy-to-noise ratio ($Eb\ No$) in dB. In this case, the start of the FFT is chosen 6 points away from the region between the end of the CP and the length of the channel impulse response. The simulation was run for 20,000 symbols with QPSK modulation.

The data points on the plots are connected with a line. It can clearly be seen that early timing degrades the BER. For the same BER, the case with early synchronization requires about 0.5 dB more energy than the case with correct timing.
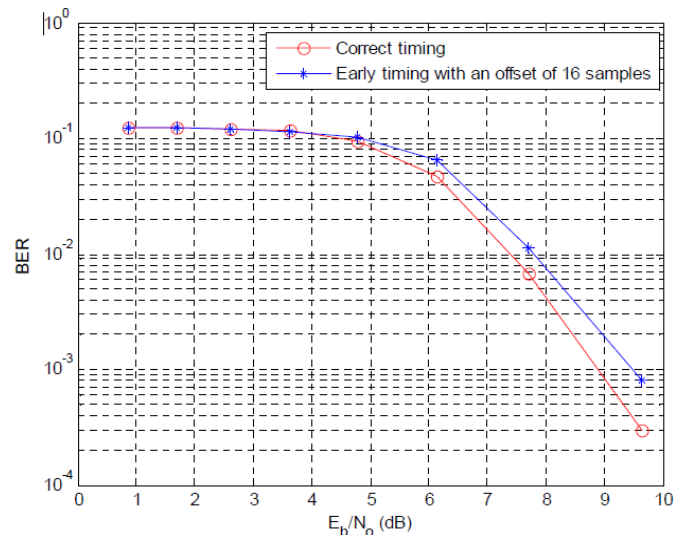

Figure3. The effects of ISI and ICI due to early timing

The effect of ISI and ICI due to late timing, however, can be more destructive than early timing since, in the case of late timing, the OFDM symbol includes samples from the CP of the next OFDM symbol. This effect can be thought of as a burst error. Figure 4 presents BER versus bit energy-to-noise ratio ($E_b\ N_o$) plots for correct timing and timing offset of 100 ns with QPSK modulation. The simulation was run for 20,000 symbols. The data points on the plots are connected with a line. It can be observed from the figure that the BER plot for this late timing is as much as 2 dB worse than the BER plot for correct timing.
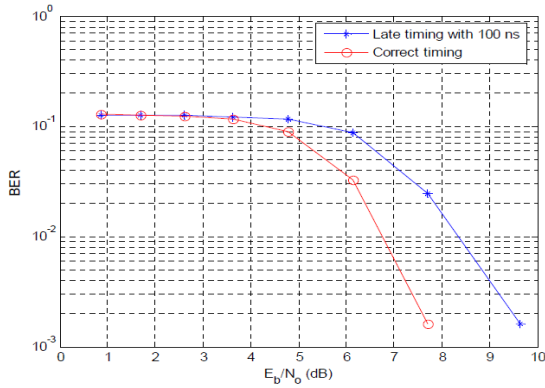
Figure 4. The effects of ISI and ICI due to late timing

FINE TIMING

In this section, the fine timing methods of interest are described. In all, three timing methods are introduced.

Method 1: Schmidl and Cox Method

In Schmidl and Cox method [vii], timing synchronization is achieved by using a training sequence whose first half is equal to its second half in the time domain. The basic idea behind the technique is that the symbol timing errors will have little effect on the signal itself as long as the timing estimate is in the CP.

The two halves of the training sequence are made identical by transmitting a PN sequence on the even frequencies while zeros are sent on the odd frequencies. When we take the IFFT of this sequence, the property of being identical can be seen. Another way of achieving this training symbol with two identical halves is to use a PN sequence of half the symbol length (32 points for the case of IEEE 802.11a), take the IFFT of it, and then repeat it. As stated in [vii], one advantage of sending zeros on odd frequencies is that, especially in continuous broadcasting systems like DVB, this property could be used to distinguish the training symbol from the data since the data would have values on the odd frequencies. Table 1 shows a PN sequence for the training symbol. However, in [vii], a different PN sequence whose values are taken from a 64-QAM constellation is used.

Table 1. PN Sequence for Training Symbol for the Method in [vii]

Frequency Number	PN Sequence
0	$1+1*i$
1	0
2	$-1+1*i$
3	0
4	$1+1*i$
5	0
6	$1-1*i$
7	0
8	$1+1*i$
9	0

Let N be the number of complex samples in one OFDM symbol. The algorithm defined in [vii] has three steps, based on the following equations:

$$P(n) = \sum_{k=0}^{\left(\frac{N}{2}\right)-1} \left(r(n+k)^* r\left(n+k+\frac{N}{2}\right) \right) \quad \dots \quad (1)$$

$$R(n) = \sum_{k=0}^{\left(\frac{N}{2}\right)-1} \left| r\left(n+k+\frac{N}{2}\right) \right|^2 \quad \dots \quad (2)$$

$$M(n) = \frac{|P(n)|^2}{\left(R(n)\right)^2} \quad \dots \quad (3)$$

In Equation 1, the algorithm has a window length of N, which is also the number of sub-carriers. The starting point is the value of n, which maximizes $M(n)$. In fact, from the definition, $P(n)$ expresses the cross-correlation between the two halves of the window; in Equation 2, $R(n)$ represents the auto-correlation of the second half. When the starting point of the window reaches the start of the training symbol with the CP, the values of $P(n)$ and $R(n)$ should be equal giving the maximum value for the timing metric as defined in Equation 3.

Under ideal conditions, when there is no channel effect and no noise, the timing metric gives a plateau of width equal to the CP. In order to see how the algorithm works, we implemented the algorithm and obtained the timing metric. Figure 5 shows the timing metric under ideal channel conditions. It is obvious that the plateau starts at the sample 81, which is the starting point of the CP, and the plateau runs till the sample 97, which is the start of the symbol. The length of the plateau should reduce down to the CP minus the length of the channel impulse response under the actual conditions.
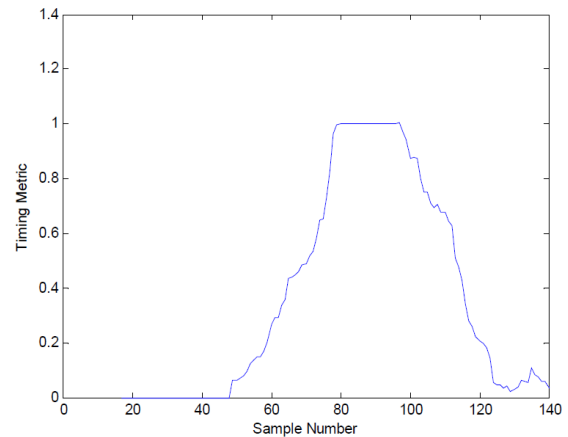

Figure 5. Timing Metric for Schmidl and Cox Method under Ideal Conditions with No Channel Effect and No Noise

Method 2: Minn and Bhargava Method

In [viii], Minn and Bhargava present another method to reduce the uncertainty that [vii] has in finding the correct timing. They propose an OFDM training symbol to be of the form given by

$$\mathbf{s} = [\ S/4 \ \ S/4 \ \ -S/4 \ \ -S/4 \ ]$$

where $S/4$ represents the $N/4$ point IFFT of a modulated PN sequence. The chosen PN sequence is given in Table 2 :

Table 2. PN Sequence to Obtain the Training Symbol in [8]

Frequency Number	PN Sequence
0	$1+1*i$
1	$-1+1*i$
2	$-1-1*i$
3	$1-1*i$
4	$1+1*i$
5	$1-1*i$
6	$-1+1*i$
7	$-1+1*i$
8	$-1+1*i$
9	$1-1*i$
10	$1+1*i$
11	$1-1*i$
12	$1-1*i$
13	$-1+1*i$
14	$1+1*i$
15	$-1+1*i$

The cross-correlation sequence between the positive-valued and negative-valued parts of the training symbol is given by

$$P_2(n) = \sum_{k=0}^{1}\sum_{m=0}^{L-1} r^*(n + 2Lk + m)\, r(n + 2Lk + m + L) \quad \cdots \quad (4)$$

The auto-correlation sequence of the second positive-valued and negative-valued parts of the symbol:

$$R_2(n) = \sum_{k=0}^{1}\sum_{m=0}^{L-1} |\, r(n + 2Lk + m + L)|^2 \quad \cdots \quad (5)$$

where L is the length of $S/4$. Finally, the timing metric is given by

$$M_2(n) = \frac{|P_2(n)|^2}{(R_2(n))^2} \quad \cdots \quad (6)$$

Equation 5 basically calculates half symbol energy using $N/2$ samples. This equation can be replaced by

$$R_2(n) = \frac{1}{2}\sum_{m=0}^{N-1} |\, r(n + m)|^2 \quad \cdots \quad (7)$$

The idea behind this method is to avoid the plateau we found in [vii] and shown in Figure 5. Another point to note is that the results are based on 1,024 sub-carriers and 10% of the OFDM symbol as CP, which corresponds to 102 samples. This technique is not directly applicable to IEEE 802.11a since there are only 64 sub-carriers and the CP is 16 samples that correspond to one-fourth of the OFDM symbol itself. In the simulations, we did not add the CP. Adding the CP causes the timing metric to have more peaks.

Figure 6 shows the timing metric under ideal channel conditions. The middle peak is the peak of interest. In this simulation, the starting point of the training symbol is sample 96, where the timing metric has a peak with the magnitude of 1.
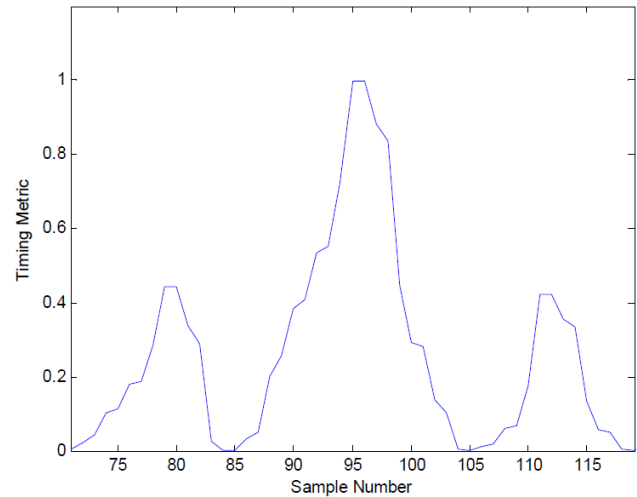

Figure 6. Timing Metric for Minn and Bhargava Method [8] under Ideal Conditions with No Channel Effect and No Noise

Method 3: Park et al. Method

The third method we studied was proposed by Park et al. [ix]. The training symbol used in this method is given by

$$s = [\ S/4 \quad A/4^* \quad S/4 \quad A/4^* \ ]$$

where $S/4$ represents time samples of length $N/4$ formed by IFFT of a PN sequence, $A/4_*$ represents the time-reversed conjugate of $S/4$.

This symbol can easily be obtained by having a real-valued PN sequence on the even frequencies and zeros on the odd frequencies and applying the IFFT operation to this sequence. A new algorithm is proposed to exploit the symmetric property of the above training symbol. The cross correlation sequence, the auto-correlation sequence, and the timing metric, respectively are given by

$$P_3(n) = \sum_{k=0}^{\frac{N}{2}} (r(n - k)\, r(n + k)) \quad \cdots \quad (8)$$

$$R_3(n) = \sum_{k=0}^{N/2} |r(n + k)|^2 \quad \cdots \quad (9)$$

$$M_3(n) = \frac{|P_3(n)|^2}{(R_3(n))^2} \quad \cdots \quad (10)$$

The idea behind the symmetric property of this algorithm is to have only one mutual product for each n value. Therefore, the estimation of the timing occurs at the desired correct symbol timing while other values approach zero.

In this method, although the peak occurs exactly at the correct timing, we found that its peak magnitude is very sensitive to AWGN and indoor multi-path channels, which makes the estimation over a threshold difficult. Figure 7 presents the plot for the timing metric under ideal channel conditions.

The desired starting point is 129, and the delta function-like shape of the timing metric can clearly be seen at the exact starting point. The timing metric for this method has a narrower peak than both methods discussed earlier (see Figures 5 and 6).
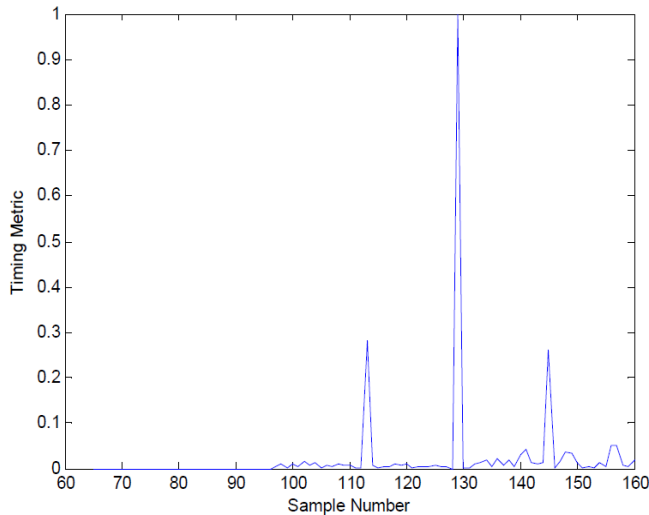
Figure 7. Timing Metric for Park et al. Method under Ideal Conditions with No Channel Effect and No Noise

III. Results and Tables
Comparison of the Timing Methods

We present two tables summarizing the results of the simulations. Table 3 gives the information among 3 methods for their desired point of starting and actual point of starting , Whether Table 4 evaluates ease of implementation .
The evaluations are inferred from the simulations results.

Table 3 : Starting Points

Method\Points	Desired starting point	Actual starting point
1. Schmidl and Cox	100	81
2. Minn and Bhargava	100	96
3. Park et al.	129	129

Table 4 : Ease of implementation

Method\Condition	Indoor	Outdoor	AWGN	Implemen tation
1. Schmidl and Cox	Poor	Good	Poor	Poor
2. Minn and Bhargava	Good	Good	Good	Poor
3. Park et al.	Good	Fairly Good	Poor	Good

For the Schmidl and Cox method, we discovered that the plateau inherent in the method raises uncertainty in the timing distribution. The timing distribution may span as many as 8 samples. The edge of the timing metric plateau changes depending on the multi-path, noise power, and delays, which makes the implementation very difficult. Another disadvantage is the question of finding the optimum timing point. However, there are other studies showing some advantages of this method. For example, [x] shows that Schmidl and Cox method is very robust against carrier frequency
offset and fading.
The Minn and Bhargava method successfully avoids the disadvantages of the Schmidl and Cox method. It does not have a plateau, and the variance of the estimator is lower. Nevertheless,

in order to reach this conclusion, we assumed that the middle peak always has larger amount of energy than the other peaks on both sides.
The main disadvantage that we noted about the Park et al. method is that it is very sensitive to AWGN. However, it is worth noting that the peaks due to correlation with noise and data sent after the training symbol do not quickly go up. This improves the performance of the method. For relatively high values of E_bN_o , this method is robust in outdoor channels whereas the timing distribution has a tendency to worsen in indoor channels.

IV. Conclusion

In this paper, we presented the need for timing synchronization, the methods used for timing synchronization and their comparison. We also provided the performance plots for algorithms in a noise-free environment without any channel effects. In this way we have seen that Park et al. method is the best among all three methods due to high values of $E_b N_o$ and where desired and actual starting points are the same at 129.

References

i.   Y.Wu and W. Y. Zou, "Orthogonal frequency division multiplexing: A multi-carrier modulation scheme," IEEE Trans. Consumer Electronics, vol. 42. no. 3, pp. 392-399, August 1995.

ii.   W. Y. Zou and Y. Wu, "COFDM: An overview," IEEE Trans. Broadcasting, vol. 41 no.1, pp. 1-8, March 1995.

iii.   Jae Hong Lee Seung Hee Han, "An Overview Of Peak-To-Average Powerratio Reduction Techniques For Multicarrier Transmission," IEEE WirelessCommunications, pp. 56-65, April 2005.

iv.   Yiyan Wu Tao Jiang, "An Overview: Peak-to-Average Power Ratio Reduction Techniques for OFDM Signals," IEEE TRANSACTIONS ON BROADCASTING, VOL. 54, NO. 2, JUNE 2008, vol. 54, no.2, pp. 257-268, June 2008.

v.   Young-Jae Ryu and Dong-Seog Han, "Timing phase estimator overcoming Rayleigh fading for OFDM systems," IEEE Transactions on Consumer Electronics, vol. 47, no. 12, pp. 370-377, Aug. 2001.

vi.   L. Hazy and M. El-Tanany, "Synchronization of OFDM systems over frequency selective fading channels," IEEE 47th Vehicular Technology Conference, vol. 3, pp. 2094-2098, May 1997.

vii.   Timothy M. Schmidl and Donald C. Cox, "Robust frequency and timing synchronization for OFDM," IEEE Trans. on Commun., vol. 45, no. 12, pp. 1613-1621,Dec. 1997.

viii.   H. Minn and V. K. Bhargava, "A simple and efficient timing offset estimation for OFDM systems," IEEE 51st Vehicular Technology Conference Proceedings, vol. 1, pp. 51-55, May 2000.

ix.   Byungjoon Park, Hyunsoo Cheon, Changeon Kang and Daesik Hong, "A nove timing estimation method for OFDM systems," IEEE Commun. Letters, vol. 7, no. 15, pp. 239-241, May 2003.

x.   Luc Deniere, Wireless OFDM Systems: How to Make Them Work, Mark Engels,ed., Chapter 6, pp.95-111, Kluwer Academic Publishers, Dordrecht, The Netherlands 2002